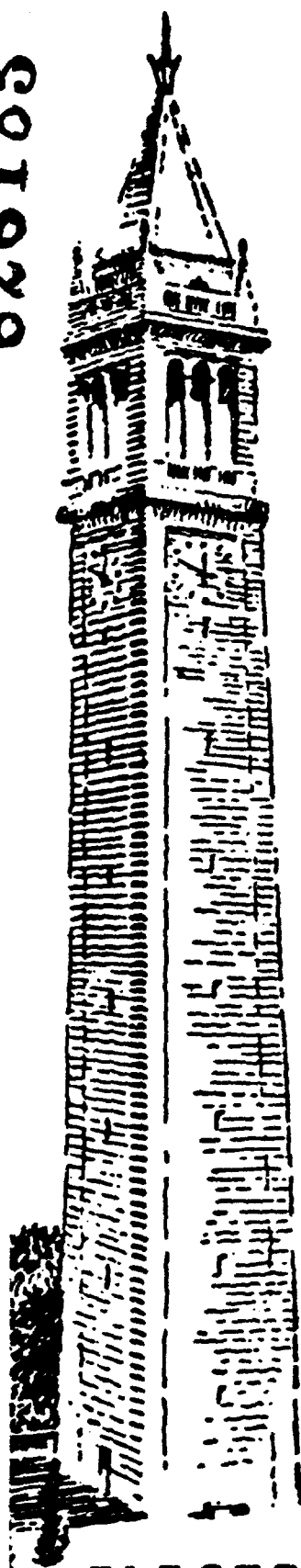


626183



CLEARINGHOUSE FOR FEDERAL SCIENTIFIC AND TECHNICAL INFORMATION		
Hardcopy	Microfilm	
\$1.00	\$0.50	25.00
ARCHIVE COPY		

000001

STUDY OF CROSSED-FIELD AMPLIFIERS

Report Nr. 8
Contract Nr. DA 36-039 AMC-02164(E)
DA Task Nr. 3A99-13-001

Eighth Quarterly Progress Report
15 April - 15 June 1965

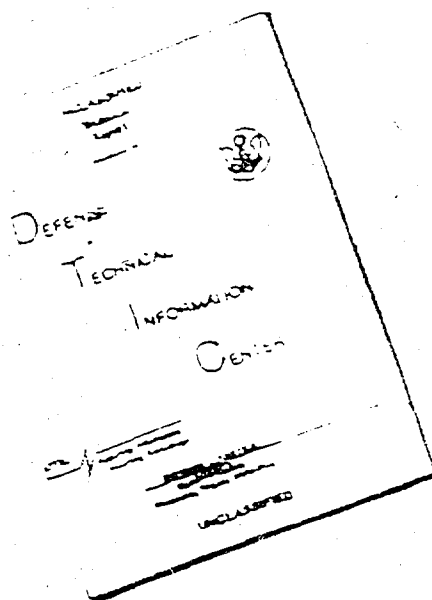
United States Army Electronics Command
Fort Monmouth, New Jersey

ELECTRONICS RESEARCH LABORATORY

UNIVERSITY OF CALIFORNIA

BERKELEY, CALIFORNIA

DISCLAIMER NOTICE



THIS DOCUMENT IS BEST
QUALITY AVAILABLE. THE COPY
FURNISHED TO DTIC CONTAINED
A SIGNIFICANT NUMBER OF
PAGES WHICH DO NOT
REPRODUCE LEGIBLY.

THIS DOCUMENT CONTAINED
BLANK PAGES THAT HAVE
BEEN DELETED

REPRODUCED FROM
BEST AVAILABLE COPY

This Document Contains
Missing Page/s That Are
Unavailable In The
Original Document

STUDY OF CROSSED-FIELD AMPLIFIERS

Report Nr. 8
Contract Nr. DA 36-039 AMC-02164(E)
DA Task Nr. 3A99-13-001

Eighth Quarterly Progress Report
15 April - 15 June 1965

ELECTRONICS RESEARCH LABORATORY
University of California, Berkeley

ABSTRACT

An electron gun which produces a smooth transition from Kino flow near the drift region was designed using a new method of synthesis. An experimental gun was fabricated and tested. The agreement between theory and experiment was good. Noise-figure expressions were derived for cyclotron and space-charge wave amplifiers. These expressions are to be studied to determine the conditions for minimum noise-figure. A five-wave analysis was used to determine the wave amplitudes and phase factors resulting from the interaction between the circuit wave and the beam space-charge waves. The amplitudes of the significant waves were calculated as a function of beam position for normal experimental conditions. Calculations show that beam-position fluctuation is the most important factor in the noise-figure.

A theoretical analysis of crossed-field guns is being carried out to study the effect of a crossed magnetic field on potential minimum stability. A statistical analysis of the cut-off characteristics of the smooth-bore magnetron was completed. The theoretical results were shown to be in close agreement with existing experimental results.

TABLE OF CONTENTS

SHIELDED-GUN LOW NOISE AMPLIFIER	1
FORWARD-WAVE NOISE FIGURE STUDIES	2
BACKWARD-WAVE NOISE FIGURE STUDIES	3
CATHODE-REGION STUDIES ON CROSSED-FIELD TUBES	11
CHARACTERISTICS OF THE SMOOTH-BORE MAGNETRON	14
REFERENCES	19

ELECTRONICS RESEARCH LABORATORY

University of California
Berkeley, California

Quarterly Progress Report
June 15, 1965

Study of Crossed-Field Amplifiers
DA 36-039 AMC-02164(E)

SHIELDED-GUN LOW NOISE AMPLIFIER

(R. A. Rao and Professor T. Van Duzer and Dr. S. P. Yü)

The objective of this project is to design a low noise shielded-gun amplifier.

As a part of the project, a method for synthesizing crossed-field electron guns has been developed. The method uses the first-order paraxial ray equation for the synthesis of the electron beam and the method of analytic continuation for the design of electrodes. An electron gun which produces a smooth transition from kino flow near the cathode to Brillouin flow near the drift region has been synthesized by this method. During this quarterly period this gun was fabricated and tested. Fig. 1 shows the electron beam and the electron gun obtained by this method of synthesis. Fig. 2 shows the assembled tube. The special features of the tube are the use of a palladium leak and an ion pump to introduce controlled amounts of hydrogen gas into the tube and the use of transparent transverse focusing electrodes to facilitate viewing of the beam. The experimental results are compared with the theory in Table I. The agreement between the theory and the experiment is good.

In order to observe the beam, a small amount of hydrogen gas was introduced into the tube through the palladium leak and the pressure inside the tube was maintained between 10^{-6} and 10^{-5} mm of mercury. At this pressure, the beam appears bright enough for viewing and photographing. Wightman¹ has shown that under conditions similar to the operating conditions of our tube, the number of ions present in the region

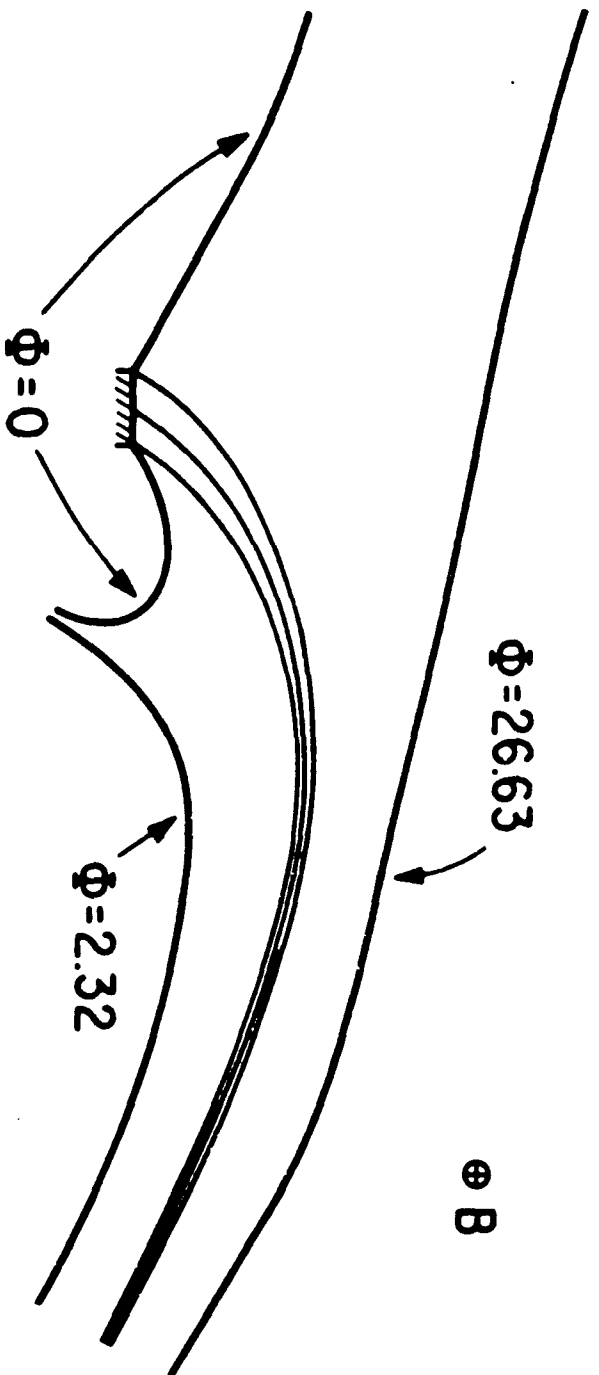


Fig. 1. Electrodes for newly synthesized beam.

of the beam is only a few percent of the number of electrons and hence the space-charge conditions are altered very little because of the ionization of hydrogen. Moreover, the uncertainty in the beam position is small enough for accurate measurements of dimensions of the order of 1 mm. This method should give an accurate representation of the actual shape of the beam. The observed beam shape seems to be qualitatively in agreement with the design values. However, for quantitative comparisons, a number of pictures of the beam were taken. The hot cathode produced too much light and this stray light tended to mask the beam near the cathode. The camera alignment was also found to be critical for obtaining an accurate value for the beam thickness. The quality of the pictures obtained so far has not been good. Meanwhile, the tube developed a crack because of the overheating of the ion pump cathode and had to be repaired. While the tube was being repaired, the computer programs for the design of the shielded-gun tube were debugged and some initial results were obtained on the shielded-gun design.

The tube is now back from the workshop and the experiments will be resumed. Narrow-band filters will be used to cut down the light from the hot cathode. The design of the shielded-gun tube will be continued.

FORWARD-WAVE NOISE FIGURE STUDIES

(A. Sasaki and Professor T. Van Duzer and Dr. S. P. Yu)

The aim of this work is to develop understanding of the noise characteristics of forward-wave crossed-field amplifiers to a sufficient degree to permit appreciable noise-figure reductions. The normal mode approach will be used in the study of noise transducing schemes.

During this quarter, the noise-figure expressions for the cyclotron and space-charge wave amplifiers were derived in terms of the normal mode amplitudes of the noise quantities at the entrance plane to the interaction region. The expressions obtained are applicable to either the forward- or backward-wave amplifier if we use the proper power gain in the expressions. The expression for the cyclotron-wave amplifier is

$$NF = 1 + \frac{|a|^2}{kT} \left(1 - \frac{1}{G}\right),$$



Fig. 2. The experimental tube.

TABLE I

COMPARISON OF THEORY AND EXPERIMENT

PARAMETERS	THEORY	EXPERIMENT
Cathode width	0.2 in.	0.2 in.
Anode width	infinite	1.5 in.
Drillouin thickness	0.0363 in.	-
Magnetic field	70.5 gauss	72 gauss ($\pm 2\%$)
Anode potential	1500 volts	1500 volts ($\pm 2\%$)
Cole potential	131 volts	131 volts ($\pm 2\%$)
Circuit potential	1500 volts	1450 volts ($\pm 2\%$)
Cathode current	47.2 ma	52.0 ma ($\pm 2\%$)
Transmission to collector	100%	99%

where $|a|^2$ is the absolute value of noise power carried by the slow cyclotron wave, G is the power gain of the amplifier, k is Boltzman's constant, and T is room temperature. The expression for the space-charge wave amplifier is

$$Nf = 1 + \frac{1}{2kT} |Pa_g - Qa_d|^2 (1 - \frac{1}{G}),$$

where

$$P = S_g^2 + 1 + S_g,$$

$$Q = S_g^2 + 1 - S_g,$$

$$S_g^2 = S^2 \frac{G - 1}{G + 1}.$$

Here, S is the space-charge parameter in Gould's notation, a_g and a_d are the normal mode amplitudes of the growing and decaying waves due to the beam noise at the entrance plane to the interaction region. In the coming period, the minimum noise-figure expression of a crossed-field amplifier will be studied.

BACKWARD-WAVE NOISE FIGURE STUDIES

(N. R. Mantena and Professor T. Van Duzer and Dr. S. P. Yü)

The objective of this project is to identify and reduce excess noise in crossed-field amplifiers. This report deals with the theoretical justification of the experimental results presented in the previous quarterly reports.

Following Hutter's five-wave analysis², the amplitude and phase factors of all the five waves resulting from the interaction between the circuit wave and the beam space-charge waves can be determined. These are given from the following set of linear equations:

$$\begin{pmatrix} E_{1zt} \\ \sigma_{1t} \\ y_{1t} \\ v_{lyt} \\ v_{lzt} \end{pmatrix} = \begin{pmatrix} \alpha_{11} & \alpha_{12} & \alpha_{13} & \alpha_{14} & \alpha_{15} \\ \alpha_{21} & \alpha_{22} & \alpha_{23} & \alpha_{24} & \alpha_{25} \\ \alpha_{31} & \alpha_{32} & \alpha_{33} & \alpha_{34} & \alpha_{35} \\ \alpha_{41} & \alpha_{42} & \alpha_{43} & \alpha_{44} & \alpha_{45} \\ \alpha_{51} & \alpha_{52} & \alpha_{53} & \alpha_{54} & \alpha_{55} \end{pmatrix} \begin{pmatrix} E_1 \\ E_2 \\ E_3 \\ E_4 \\ E_5 \end{pmatrix} \quad (1)$$

where E_{1zt} is the longitudinal component of the circuit electric field; σ_1 , y_1 , v_{ly} , and v_{lz} are, respectively, the fluctuations in the surface-charged density, the transfer beam position, and the two velocity components at the interaction entrance plane; "t" refers to the total quantities; E_i | $i=1$ to 5 are the amplitudes of the modified circuit wave, the two modified beam space-charge waves, and the two cyclotron waves at the circuit plane of the interaction input plane; α_{ij} are complicated functions of Gould's parameters g, d, b, D, S . The incremental propagation constants δ_i are defined below.

For the modified circuit and space-charge waves

$$\beta_i = \frac{\omega}{u_0} (1 + jD\delta_i), \quad i = 1 \text{ to } 3, \quad (2)$$

and for the cyclotron waves,

$$\begin{aligned} \beta_4 &= \frac{(\omega + \omega_c)}{u_0} (1 + jD_4\delta_4), \\ \beta_5 &= \frac{(\omega - \omega_c)}{u_0} (1 + jD_5\delta_5), \end{aligned} \quad (3)$$

δ_1, δ_2 , and δ_3 are determined from the determinantal equation

$$(\delta + jb \pm d)(\delta^2 + j2gS\delta - S^2) = \pm \delta, \quad (4)$$

where the upper and lower signs refer to the circuit forward and backward wave interactions; δ_4 and δ_5 have been determined to be

$$\delta_4 = j \left[\frac{e^{-(\beta_e + \beta_m)(a-d)}}{\sinh(\beta_e + \beta_m)(a+d)} - \frac{D_4 S_4}{2} \frac{\beta_e + \beta_m}{\beta_m} \right] S_4 \quad (5)$$

and

$$\delta_5 = -j \left[\frac{e^{-(\beta_e - \beta_m)(a-d)}}{\sinh(\beta_e - \beta_m)(a+d)} - \frac{D_5 S_5}{2} \frac{\beta_e - \beta_m}{\beta_m} \right] S_5,$$

where $\beta_e = \frac{\omega}{u_0}$, $\beta_m = \frac{\omega}{u_0}$, and a , d are distances of the beam from the cole and circuit planes; D_4 , S_4 , and D_5 , S_5 are just like Gould's D , S but evaluated for the slow and fast cyclotron wave phase constants, $(\beta_e + \beta_m)$ and $(\beta_e - \beta_m)$. In deriving Eqs. 1, 4, and 5, the assumptions $D \ll 1$, $D\delta_i \ll 1$ have been made.

Using the parameters resulting from the experimental conditions and inverting Eq. 1 with the help of an IBM 7094, we found that the cyclotron wave amplitudes due to the circuit electric field E_{1zt} are at the most 10^{-8} times the amplitude of the growing, decaying, or constant wave. Similarly the cyclotron wave amplitude due to the beam noise quantities σ_{1t} , y_{1t} , v_{1yt} , and v_{1zt} were also found to be negligible as compared to the amplitudes of the growing, decaying, and constant wave amplitudes. Therefore, the results clearly show that the cyclotron waves, with phase velocities far different from the electron-beam velocity, do not appear either in the interaction process of the noise analysis. It is thus seen that the three waves with phase velocity near the electron-beam velocity are the most important in the interaction and noise analyses. The amplitudes of these waves as a function of normalized beam distance from the sole plate for the usual experimental conditions are shown in Fig. 1. It is interesting to note that the relative growing wave excitation follows the theoretical expression $\frac{1}{2(1+S^2)}$ in accordance with Wightman's results.³

1. Noise Figure of Forward- and Backward- Wave Amplifiers

The noise figure of either forward- or backward- wave amplifiers is expressed in terms of the mean square values of σ_1 , y_1 , v_{1y} , v_{1z} , and the mean values of cross correlation among them. It is found

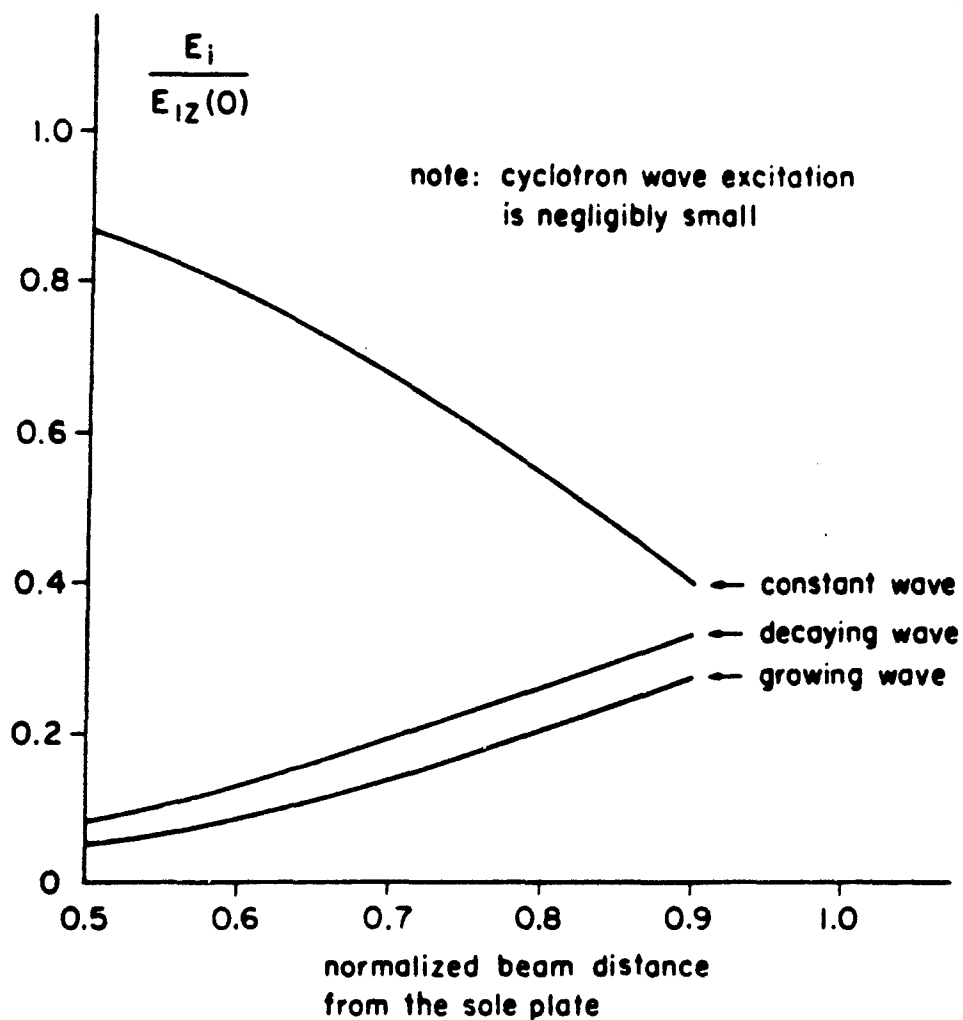


Fig. 1. Wave excitation as a function of normalized beam distance, (for $V_0 = 790$ volts, $I_0 = 130.5$ ma, $f = 1.51$ Gc, $B_0 = 232$ gauss and $K_0 = 7.2 \Omega$).

that the terms involving v_{1y} and v_{1z} make very slight contributions to the noise figure. In terms of other quantities, the noise figure F can be written as:

$$F = 1 + P_{11} \overline{\sigma_1^2(0)} + P_{12} \overline{y_1^2(0)} + P_{13} \overline{\text{Re}(\sigma_1(0)y_1^*(0))} + P_{14} \overline{\text{Im}(\sigma_1(0)y_1^*(0))}, \quad (6)$$

where (0) refers to the entrance plane of the interaction region; P_{11} , P_{12} , P_{13} , and P_{14} are complicated functions of Gould's parameters, frequency, and beam position in the interaction region. Van Duzer's model⁴ has been used to determine

$$\overline{\sigma_1^2(0)}, \overline{y_1^2(0)}, \overline{\text{Re}(\sigma_1(0)y_1^*(0))} \text{ and } \overline{\text{Im}(\sigma_1(0)y_1^*(0))}$$

starting from velocity, beam position and shot current fluctuations at the potential minimum plane, assuming zero cross correlation among them. Calculations show that the beam position fluctuations contribute most to the noise figure. For a beam (normalized) position of 0.5, the forward wave amplifier noise figure calculated from Eq. 6 is 31.24 db as compared with the experimental value of 27.2 db.

Our estimate of noise figure variation (Fig. 2) with normalized beam distance shows good qualitative agreement with experiment. By including diocotron gain change with beam position in the drift region preceding the interaction space, this qualitative agreement is greatly improved. In view of many approximations made in the gun region and drift space analyses, the quantitative agreement with experiment seems to be satisfactory. The noise figure calculations will be made for the backward wave amplifier then compared with the experimental results.

2. Space Charge Smoothing in Crossed-Field Amplifiers

Since the beam position fluctuations appear to be dominant in determining the noise figure, it seems logical to investigate whether the beam position fluctuations are smoothed by the space-charge loading of the cathode. Following Van Duzer's analysis⁴, position fluctuations have been derived assuming a smoothing factor Γ^2 for the shot current. It was found that the position fluctuations contain the same smoothing factor. This finding agrees very well with the theoretical justification

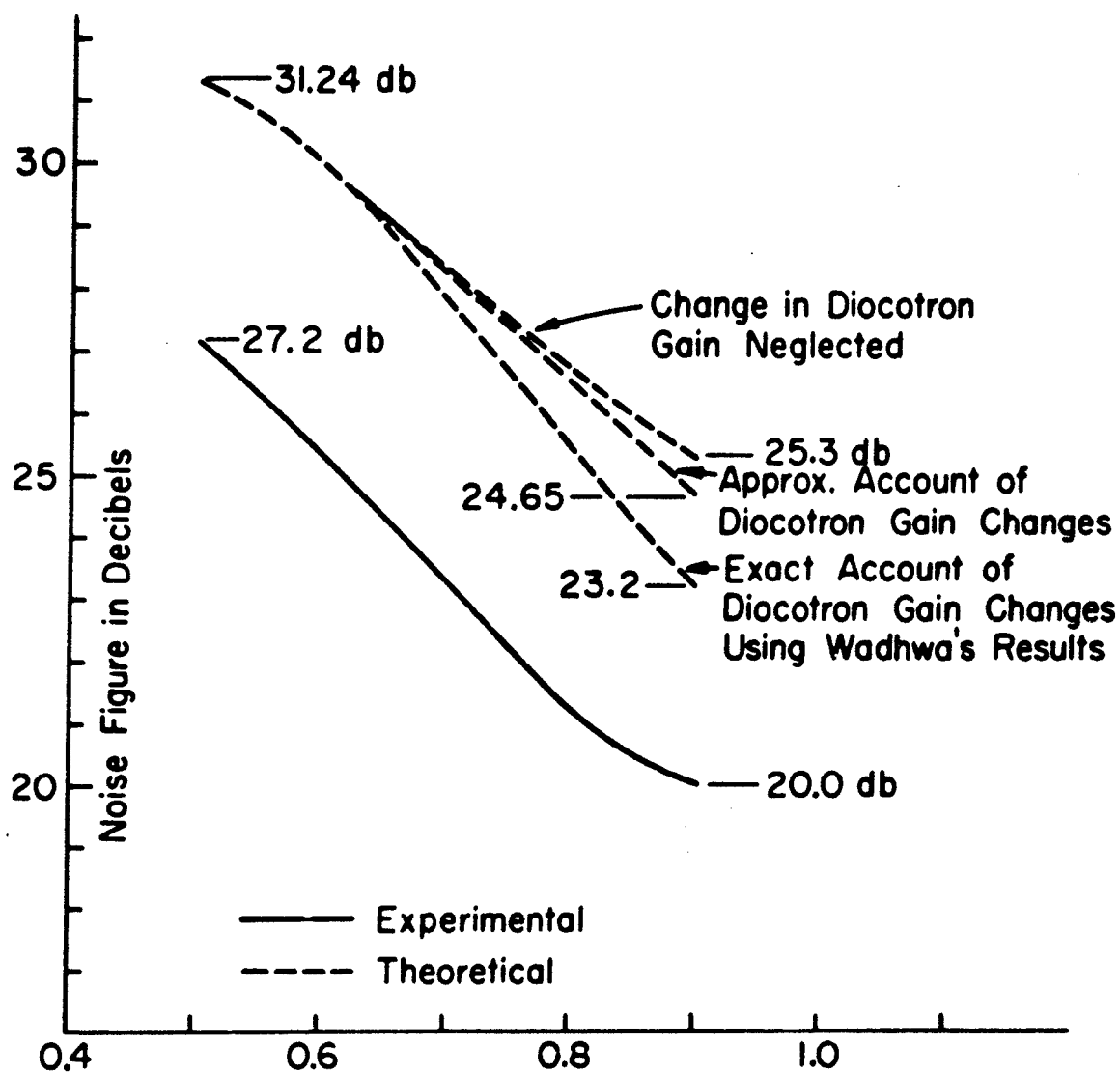


Fig. 2. Normalized beam distance $a/(a+d)$.

for space-charge smoothing obtained previously⁵. However, the reasons for larger reduction of noise figure in the BWA (about 5 db at $f=860$ Mc) as compared to 3.1 db at 1510 Mc. in the FWA will be investigated and related to the potential minimum parameter, namely, the ratio of the frequency of operation to the plasma frequency at the potential minimum.

2. Matrix Inversion Scheme to Obtain the Correlation Between Noise Quantities at the Potential Minimum

The purpose of this work is to obtain the amount of cross correlation among noise quantities at a plane immediately above the potential minimum. For this, we make use of the experimental noise figures and theoretical noise figure analysis of the interaction region as shown below. We can rewrite Eq. 6 as

$$F_i - 1 = (P_{i1} P_{i2} P_{i3} P_{i4}) \begin{bmatrix} \overline{\sigma_1^2(0)} \\ \overline{y_1^2(0)} \\ \overline{\text{Re}(\sigma_1(0)y_1^*(0))} \\ \overline{\text{Im}(\sigma_1(0)y_1^*(0))} \end{bmatrix} \quad (7)$$

where i refers to a particular beam position in the interaction space. If the beam position is changed, the elements of the row matrix also change and the column noise quantity matrix remains unchanged. For four beam positions, the (4×1) noise figure matrix is related to the (4×1) noise quantity matrix through a (4×4) "P" matrix. The noise quantity matrix can be easily obtained from Eq. 7. Similarly, the noise quantities at the potential minimum $\overline{v_{ym}^2}$, $\overline{y_m^2}$, $\overline{\text{Re}(v_{ym}y_m^*)}$, and $\overline{\text{Im}(v_{ym}y_m^*)}$

are linearly related to $\overline{\sigma_1^2(0)}$, $\overline{y_1^2(0)}$, $\overline{\text{Re}(\sigma_1(0)y_1^*(0))}$, and $\overline{\text{Im}(\sigma_1(0)y_1^*(0))}$. Having determined the noise quantities at the interaction input plane, we can now obtain the potential minimum quantities.

This analysis is being applied to the forward wave amplifier. The variation of P_{i1} , P_{i2} , P_{i3} , and P_{i4} with normalized beam distance is shown in Fig. 3 and these elements will be used to obtain the potential

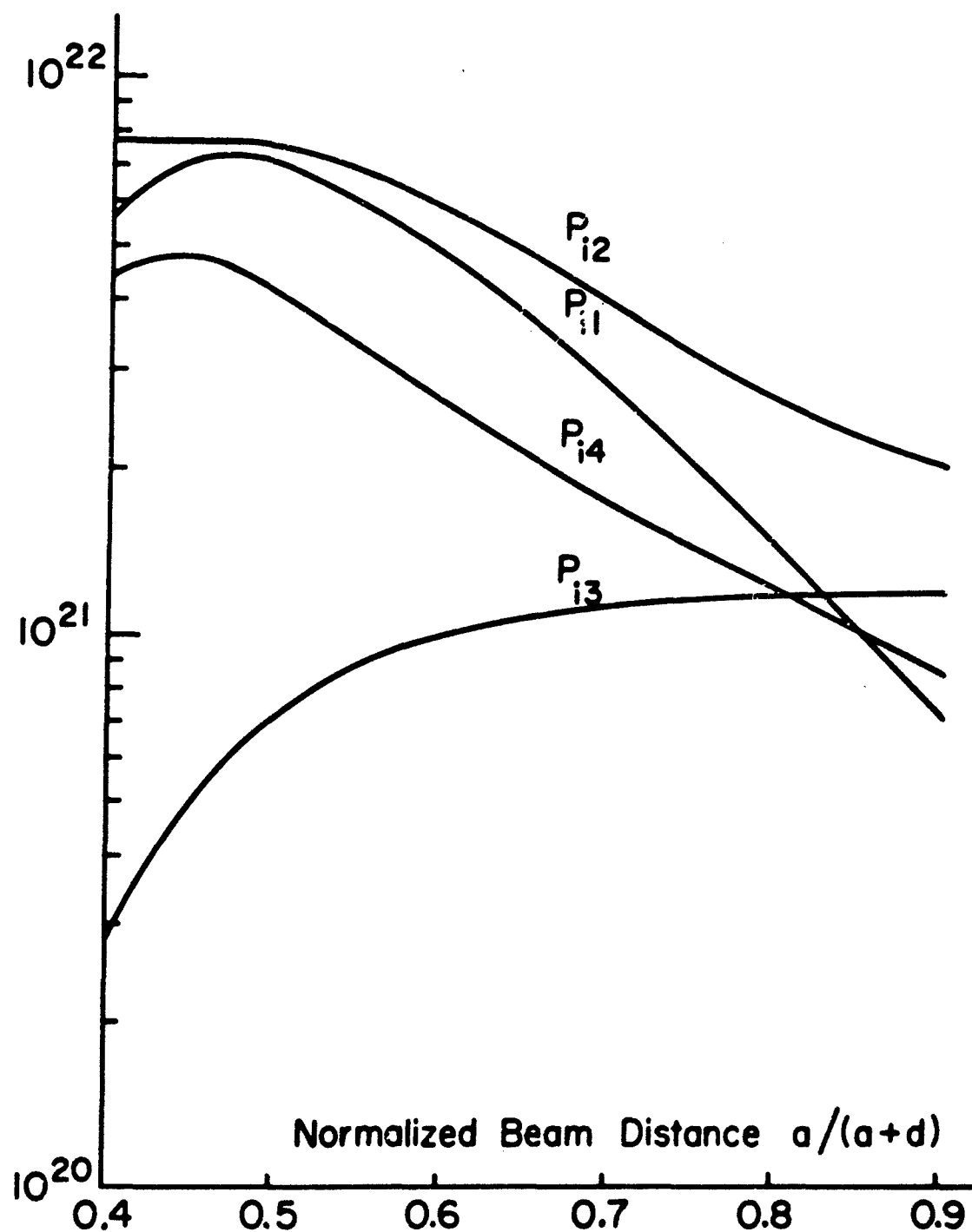


Fig. 3. Matrix elements P_{i1} , P_{i2} , P_{i3} , P_{i4} as a function of beam normalized distance from the sole plate.

quantities. It is hoped that the small discrepancy in the theoretical and experimental noise figure will be explained by finite noise correlation at the potential minimum which so far has been assumed to be zero.

Finally, the low noise figures ^{5,6} recently reported will be explained by using our theory and some general criteria for very low noise operation will be established and reported in the final report that is being written on this project.

CATHODE-REGION STUDIES ON CROSSED-FIELD TUBES

(R. Y. C. Ho and Professor T. Van Duzer and Dr. S. P. Yü)

The aim of this work is to study the effect of a crossed magnetic field on potential minimum stability.

The β -electron termination phenomenon is being studied. We assume that an equilibrium state exists in the M-diode before the perturbation current is introduced into it. The field distributions in the cathode region and beyond may be assumed to have the following forms,

$$E(y) = - \frac{2V_m}{y_m} \left(1 - \frac{y}{y_m}\right) \quad y < y_m \quad (1)$$

$$E(y) = - \frac{J}{\epsilon_0} (t - t_m) \quad y > y_m \quad (2)$$

where y is the coordinate normal to the cathode, V_m , y_m are the minimum potential parameters, J is the beam current density, and t is the transit time. With this assumed potential distribution, the trajectories of the perturbation electrons with a half-Maxwellian velocity distribution in the normal direction and a full Maxwellian velocity distribution in the transverse direction are solved, to the first order of accuracy, as

$$\begin{aligned}
y = & \frac{K}{\Omega^2} (1 - \cosh \Omega t) + \frac{\dot{y}_0}{\Omega} \sinh \Omega t \quad U(t) - U(t-t_m) \\
& + (y_m + \frac{\dot{x}_0}{\omega_c}) \cos \omega_c (t-t_m) + \frac{1}{\omega_c} (\dot{y}_m - \frac{\eta J}{\epsilon_0 \omega_c^2}) \sin \omega_c (t-t_m) \quad (3) \\
& + \frac{\eta J}{\epsilon_0 \omega_c^2} (t-t_m) - \frac{x_0}{\omega_c} \quad U(t-t_m)
\end{aligned}$$

and

$$\begin{aligned}
x-x_0 = & \frac{\omega_c K}{\Omega^2} t - \frac{K \omega_c}{\Omega^3} \sinh \Omega t + \frac{\dot{y}_0}{\Omega^2} (\cosh \Omega t - 1) + \dot{x}_0 t \quad U(t) - U(t-t_m) \\
& + x_m + (y_m + \frac{\dot{x}_0}{\omega_c}) \sin \omega_c (t-t_m) + \frac{1}{\omega_c} (\dot{y}_m - \frac{\eta J}{\epsilon_0 \omega_c^2}) (1 - \cos \omega_c (t-t_m)) \quad (4) \\
& + \frac{\eta J}{\epsilon_0 \omega_c^2} \frac{(t-t_m)^2}{2} - \dot{x}_0 (t-t_m) + \dot{x}_m (t-t_m) \quad U(t-t_m)
\end{aligned}$$

where $U(t)$ is the step function and K, Ω are the same as previously reported.

The determination of the d-c parameters in the M-diode has also been considered. It was reported⁷ that in a space-charge-limited M-diode the critical plane and the critical initial velocity pair can be expressed as

$$\frac{y_c}{y_m} = \frac{\frac{2 \eta V_m}{y_m} + \omega_c \dot{x}}{\frac{-2 \eta V_m}{y_m} - \omega_c^2 y_m} \quad (5)$$

and

$$\dot{y}_{0c} = -\frac{2\eta V_m}{\Omega y_c} + \frac{\omega_c}{\Omega} x_0 \quad (6)$$

where y_c is the position of critical plane and \dot{y}_{0c} is the critical initial velocity with respect to a transverse initial velocity \dot{x}_0 . If we combine Eqs. 5 and 6 and eliminate x_0 we may have

$$\dot{y}_{0c} = \Omega y_c' \quad (7)$$

If we plot Eqs. 6 and 7 in a phase space (y, y_0, x_0) , as shown in Fig. 1, then it shows that for an arbitrarily selected position $y = y_{c1}$ the corresponding normal critical initial velocity and transverse critical initial velocity pair are \dot{y}_{0c1} and \dot{x}_{01} respectively. If we divide the velocity plane (\dot{y}_0, \dot{x}_0) into three regions I, II, and III, as shown in Fig. 1, the space-charge density at $y = y_{c1}$ may be determined by the velocity distribution function over region I once and over region III twice, since the electrons in region III will eventually return to the

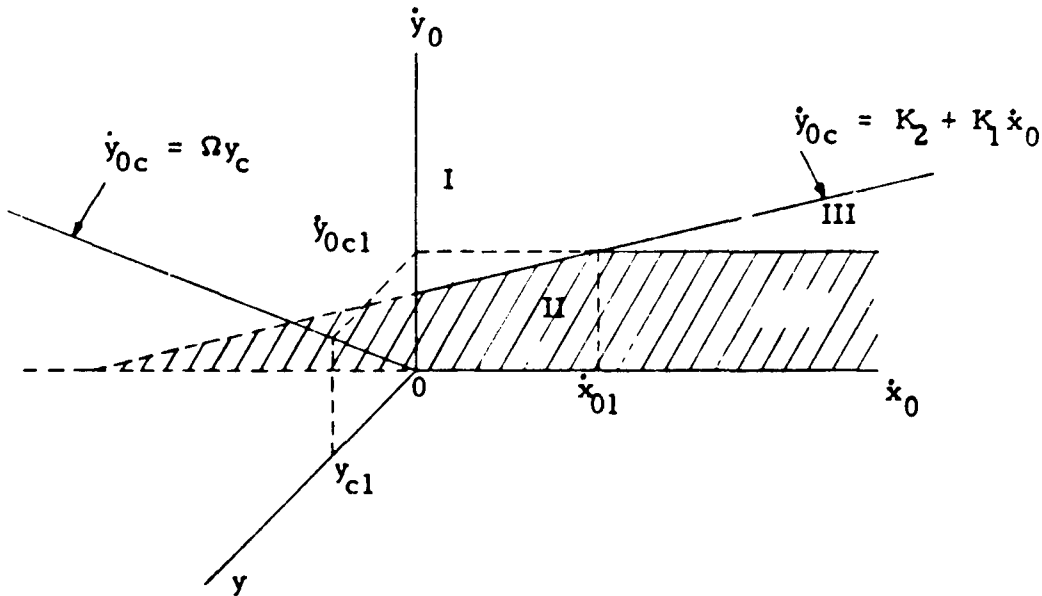


Fig. 1

cathode. Here we have assumed that the electrons after passing their critical planes will never return to the cathode. The charge density $\rho(y)$ is

$$\rho(y) = -\frac{J_s}{\sqrt{2\pi}} \left[\frac{m}{kT} \right]^{3/2} \left\{ \int_0^\infty dy_0 \int_{-\infty}^{\frac{y_0 - K_2}{K_1}} \exp - \frac{m}{2kT} (y_0^2 + x_0^2) dx_0 \right. \\ \left. + 2 \int_{\Omega_{yc}}^\infty dy_0 \int_{\frac{y_0 - K_2}{K_1}}^\infty \exp - \frac{m}{2kT} (y_0^2 + x_0^2) dx_0 \right\} \quad (8)$$

where J_s is the emission current density. We expect to form the β -electron termination model in the next quarter.

CHARACTERISTICS OF THE SMOOTH-BORE MAGNETRON

(K. Mouthaan and Professor C. Susskind)

The theoretical part of this project was completed during the past quarterly period. The objective of the theoretical analysis was to find an acceptable theoretical explanation of the cut-off characteristics of the smooth-bore magnetron. This objective was achieved, in that the theoretical results, particularly those for the anode current, agree with existing experimental results considerably better than do the theoretical results obtained by previous investigators. A final report on the theoretical analysis is ready for printing.

To find further experimental confirmation of the theoretical results for the anode current, a medium-power smooth-bore magnetron is being built. It is hoped that experimental results will be obtained during the next quarterly period.

References

1. B. A. Wightman, "An Investigation of the Magnetron Amplifier, " Technical Report No. 52, Stanford Electronics Laboratories, Stanford, p. 83; February 9, 1959.
2. R. G. E. Hutter, "Beam and Wave Electronics in Microwave Tubes, " D. Van Nostrand Co., Inc., Princeton, N. J.; 1960.
3. Op. cit. B. A. Wightman.
4. T. Van Duzer, "Noise Figure Calculations for Crossed-Field Forward-Wave Amplifiers, " IEEE Trans. on Electron Devices, Vol. ED-10, No. 6; November 1963.
5. N. R. Mantena and T. Van Duzer, "Crossed-Field Backward-Wave Amplifier Noise Figure Studies, " Journal of Electronics and Control, Vol. 17, No. 5, p. 497; November 1964.
6. R. P. Wadhwa and T. Van Duzer, "A 3.5 db Noise-Figure, S-Band, Medium Power, Forward-Wave, Injected-Beam Crossed-Field Amplifier, " Proc. IEEE, Vol. 53, pp. 425-6; April 1965.
7. R. Y. C. Ho, "The Effect of Crossed Magnetic Field on Potential Minimum Stability, " University of California, Berkeley, ERL Technical Report No. 65-20; July 13, 1965.

UNCLASSIFIED

Security Classification

DOCUMENT CONTROL DATA - R&D

(Security classification of title, body of abstract and indexing annotation must be entered when the overall report is classified)

1. ORIGINATING ACTIVITY (Corporate author) University of California Berkeley, California		2a. REPORT SECURITY CLASSIFICATION UNCLASSIFIED	
		2b. GROUP N/A	
3. REPORT TITLE STUDY OF CROSSED-FIELD AMPLIFIERS			
4. DESCRIPTIVE NOTES (Type of report and inclusive dates) Eighth Quarterly Report - 15 April - 15 June 1965			
5. AUTHOR(S) (Last name, first name, initial) Rao, R. A.; Van Duzer, Prof. T.; Yu, Dr. S. P.			
6. REPORT DATE		7a. TOTAL NO. OF PAGES 15	7b. NO. OF REFS 7
8a. CONTRACT OR GRANT NO. DA 36-039 AWC-02164 (E)		8a. ORIGINATOR'S REPORT NUMBER(S)	
b. PROJECT NO. 3A99-13-001			
c.		8b. OTHER REPORT NO(S) (Any other numbers that may be assigned this report)	
d.			
10. AVAILABILITY/LIMITATION NOTICES Qualified requesters may obtain copies of this report from DDC. This report has been released to CFSTI.			
11. SUPPLEMENTARY NOTES		12. SPONSORING MILITARY ACTIVITY U. S. Army Electronics Command Fort Monmouth, New Jersey AMSEL-KL-TM	
13. ABSTRACT An electron gun which produces a smooth transition from Kino flow near the drift region was designed using a new method of synthesis. An experimental gun was fabricated and tested. The agreement between theory and experiment was good. Noise-figure expressions were derived for cyclotron and space-charge wave amplifiers. These expressions are to be studied to determine the conditions for minimum noise-figure. A five-wave analysis was used to determine the wave amplitudes and phase factors resulting from the interaction between the circuit wave and the beam space-charge waves. The amplitudes of the significant waves were calculated as a junction of beam position for normal experimental conditions. Calculations show that beam-position fluctuation is the most important factor in the noise-figure. A theoretical analysis of crossed-field guns is being carried out to study the effect of a crossed magnetic field on the potential minimum stability. A statistical analysis of the cut-off characteristics of the smooth-bore magnetron was completed. The theoretical results were shown to be in close agreement with existing experimental results.			

UNCLASSIFIED

Security Classification

14. KEY WORDS	LINK A		LINK B		LINK C	
	ROLE	WT	ROLE	WT	ROLE	WT
Crossed-field amplifier Crossed-field guns Noise Smooth-bore magnetron						

INSTRUCTIONS

1. **ORIGINATING ACTIVITY:** Enter the name and address of the contractor, subcontractor, grantee, Department of Defense activity or other organization (*corporate author*) issuing the report.

2a. **REPORT SECURITY CLASSIFICATION:** Enter the overall security classification of the report. Indicate whether "Restricted Data" is included. Marking is to be in accordance with appropriate security regulations.

2b. **GROUP:** Automatic downgrading is specified in DoD Directive 5200.10 and Armed Forces Industrial Manual. Enter the group number. Also, when applicable, show that optional markings have been used for Group 3 and Group 4 as authorized.

3. **REPORT TITLE:** Enter the complete report title in all capital letters. Titles in all cases should be unclassified. If a meaningful title cannot be selected without classification, show title classification in all capitals in parentheses immediately following the title.

4. **DESCRIPTIVE NOTES:** If appropriate, enter the type of report, e.g., interim, progress, summary, annual, or final. Give the inclusive dates when a specific reporting period is covered.

5. **AUTHOR(S):** Enter the name(s) of author(s) as shown on or in the report. Enter last name, first name, middle initial. If military, show rank and branch of service. The name of the principal author is an absolute minimum requirement.

6. **REPORT DATE:** Enter the date of the report as day, month, year, or month, year. If more than one date appears on the report, use date of publication.

7a. **TOTAL NUMBER OF PAGES:** The total page count should follow normal pagination procedures, i.e., enter the number of pages containing information.

7b. **NUMBER OF REFERENCES:** Enter the total number of references cited in the report.

8a. **CONTRACT OR GRANT NUMBER:** If appropriate, enter the applicable number of the contract or grant under which the report was written.

8b, 8c, & 8d. **PROJECT NUMBER:** Enter the appropriate military department identification, such as project number, subproject number, system numbers, task number, etc.

9a. **ORIGINATOR'S REPORT NUMBER(S):** Enter the official report number by which the document will be identified and controlled by the originating activity. This number must be unique to this report.

9b. **OTHER REPORT NUMBER(S):** If the report has been assigned any other report numbers (*either by the originator or by the sponsor*), also enter this number(s).

10. **AVAILABILITY/LIMITATION NOTICES:** Enter any limitations on further dissemination of the report, other than those

imposed by security classification, using standard statements such as:

- (1) "Qualified requesters may obtain copies of this report from DDC."
- (2) "Foreign announcement and dissemination of this report by DDC is not authorized."
- (3) "U. S. Government agencies may obtain copies of this report directly from DDC. Other qualified DDC users shall request through _____."
- (4) "U. S. military agencies may obtain copies of this report directly from DDC. Other qualified users shall request through _____."
- (5) "All distribution of this report is controlled. Qualified DDC users shall request through _____."

If the report has been furnished to the Office of Technical Services, Department of Commerce, for sale to the public, indicate this fact and enter the price, if known.

11. **SUPPLEMENTARY NOTES:** Use for additional explanatory notes.

12. **SPONSORING MILITARY ACTIVITY:** Enter the name of the departmental project office or laboratory sponsoring (paying for) the research and development. Include address.

13. **ABSTRACT:** Enter an abstract giving a brief and factual summary of the document indicative of the report, even though it may also appear elsewhere in the body of the technical report. If additional space is required, a continuation sheet shall be attached.

It is highly desirable that the abstract of classified report be unclassified. Each paragraph of the abstract shall end with an indication of the military security classification of the information in the paragraph, represented as (TS), (S), (C), or (U).

There is no limitation on the length of the abstract. However, the suggested length is from 150 to 225 words.

14. **KEY WORDS:** Key words are technically meaningful terms or short phrases that characterize a report and may be used as index entries for cataloging the report. Key words must be selected so that no security classification is required. Identifiers, such as equipment model designation, trade name, military project code name, geographic location, may be used as key words but will be followed by an indication of technical context. The assignment of links, roles, and weights is optional.